Proposal for racetrack microtrons as driver for a free electron laser and as injector for an electron storage ring

J.I.M. BOTMAN, W. VAN GENDEREN, H.L. HAGEDOORN, J.A. VAN DER HEIDE, W.J.G.M. KLEEVEN
Eindhoven University of Technology
G.J. ERNST, W.J. WITTEMAN
Twente University, The Netherlands

Abstract

Two similar racetrack microtrons are proposed to drive a free electron laser, and alternatively to inject into an electron storage ring. It is a joint project of two Dutch technical universities with the aim to construct a microtron for each, with different applications. The free electron laser will operate in the infrared with high power output. As injector the other microtron will serve the proposed 300 MeV electron storage ring EUTERPE. The microtron design output characteristics are: energy 25 MeV, micropulse 10 deg of the RF frequency of 3 GHz. Our aim is to come beyond the present state of the art with the following characteristics: relative energy spread 0.001, emittance 3 mm mrad, current in the micropulse 100 A subharmonic bunching at 60 MHz, macropulse length 50 μsec. A racetrack design is adopted for providing flexibility, better beam quality, and higher current in the microbunch as compared with the circular microtron. Space charge problems may be severe and have to be studied. For avoiding too heavy beam loading subharmonic bunching will be applied such that the bunches arrive in the accelerating cavity at consecutive periods of the RF wave.

Introduction

In this paper we describe aspects of two similar proposed racetrack microtrons for university laboratories. The main parameters are set by requirements for driving a free electron laser. The FEL will operate in the infrared e.g. for studies of isotope separation. Standard RF components at 3 GHz will be used. The required power will be kept low by 1 out of 46 pulse selection, which is suitable for an optical cavity length of 2.3 m. The initial repetition rate of the modulator will be 10 - 100 Hz. Typical electron energy and undulator wavelength are 25 MeV and 40 mm to provide 16 μm radiation. For this application studies of space charge effects will be crucial. Strong axial focussing will be supplied as well as means to adjust the isochronism. The other microtron will serve as injector for the proposed electron storage ring EUTERPE (1). For this purpose a higher injection energy is desirable. Therefore the microtrons will be built as constant orbit machines with variable energy up to 50 MeV. This will also supply a high power tunable light source around 4 μm.

The injector

The injector has to deliver 15-20 ps pulses with a peak current of 100 A, a repetition rate of 60 MHz and an end energy of 5 MeV. This leads to an average current in the order of 100 mA. The stable phase area of the microtron is about 30 deg and an absolute fwhm energy spread of 50 keV is allowed.
The normalized emittance of the beam has to be:

$$\epsilon_n \approx 1.5 \times 10^{-4} \text{ m.rad.}$$

At 25 MeV this gives an emittance of:

$$\epsilon = \frac{\epsilon_n}{\beta\gamma} = 3 \times 10^{-6} \text{ m.rad.}$$

This value is sufficient for a free electron laser working at a wavelength of 10 μm. The maximum allowed diameter of the beam when it enters the racetrack microtron is 3 mm. The most interesting type of injector that can meet our requirements is based on laser photo-emission (2). A photo cathode is placed inside the RF cavity and illuminated by a mode-locked frequency-doubled Nd:YAG laser with a 60 MHz repetition rate, phase-synchronised with the RF frequency. The outcoming electrons are accelerated in the cavity by about 1 MV. This leads to a very low emittance electron beam. Because for our wavelength such a very low emittance is not required we can also use a more conventional system like the one developed at Boeing (3) where, starting from a 10 A gated triode, the high current pulses can be obtained by bunching. The power required by the injector and microtron together is 100 mA x 25 MV = 2.5 MW. For such a relatively low power a macropulse as long as 50 μs can easily be obtained with for instance a Thomson TH2097 klystron.

General lay-out

The overall lay-out of the microtron is given in Fig. 1. A parameter list is given in table 1. The machine has two magnetic sectors separated by a distance of 0.5 m. This distance is suitable for the RF-cavity, injection and extraction magnets and for a small general corrector magnet. A 5 MeV injector preceeds the microtron. The orbit separation is 3 cm which is enough for placing the injector and extraction magnet. Initial parameters of these small dipoles have been calculated.

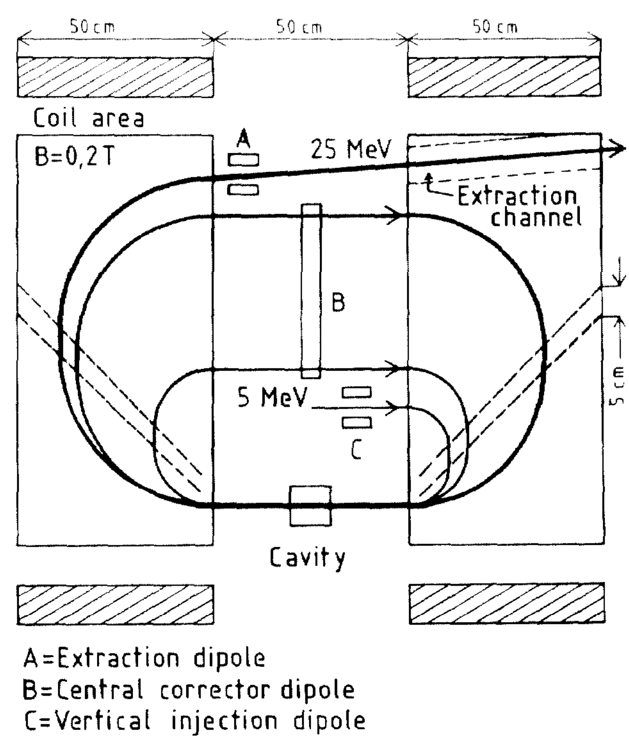

Fig. 1: Microtron lay-out.

We envisage H-type magnets providing easy accessibility from both sides. The extracted beam will leave the microtron through a channel in the righthand sector, where the field is reduced to allow proper passage. For a field of 0.2 T and 5 cm gap an excitation current is required of 4.3 kA; the magnet height is 0.5 m. Poisson calculations regarding the magnet sectors have been performed. Field clamps at the magnet entrance reduce the fringe field extension and provide a better correspondence to a hard edge model. Fig. 2 shows Poisson calculations of the field clamp effect.

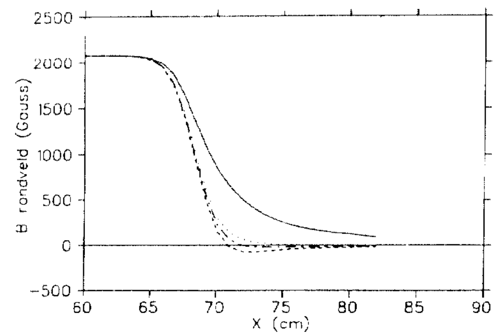

Fig. 2: Effect of field clamps at the entrance of the dipole: solid line: no field clamp, dashed lines: plus, zero, minus excitation of the field clamp.

They are not really used for axial focussing: this is achieved with 5 cm wide valleys in the pole pieces, under an angle of 45 deg with respect to the straight beam direction. Correction coils are positioned precisely in the valleys for turn by turn adjustment of the isochronism (4). A general corrector dipole in the middle of the field region will correct remaining angle deviations.

Table 1

Microtron parameter list	
Energy range	5-25 (50) MeV
Number of turns	20
Magnetic field	0.2 (0.4) T
Cavity voltage	1 (2) MV
Frequency	3 GHz
Peak current	100 A/pulse
RF power	7 MW in 50 μs
Pulse selection	1:46
Orbit separation	3 cm
Magnet sectors separation	50 cm

Axial focussing

Axial stability is obtained by edge focussing: a magnetic valley in the magnet sector pole pieces is provided under 45° with the sector edges (5). Results of hard edge stability calculations are shown in Figs. 3 and 4 for a field free valley of 5 cm orbit length: for non-accelerated orbits they display ν_r-1 and ν_z versus energy (for the end energy of 25 MeV) and the optical functions at 15 MeV. It is seen that sufficient axial focussing is achieved over the whole energy range. The beta- and dispersion functions for other energies behave in a similar fashion. The focussing system is a double achromat with zero dispersion in the cavity. In reality the valley is not field free, which reduces the axial focussing strength in particular. E.g. a valley with half the sector field (0.1 T) provides ν_z = 0.2 at 10 MeV, to be compared to 0.3 for no field. In practice the valleys will be machined as gullies in the pole pieces which are tapered and are deeper to the outside. Field measurements have to be performed.

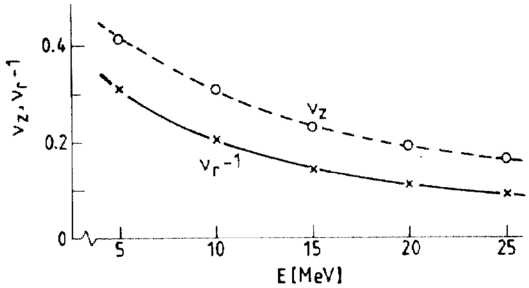

Fig. 3: Horizontal and vertical tunes for equilibrium orbits.

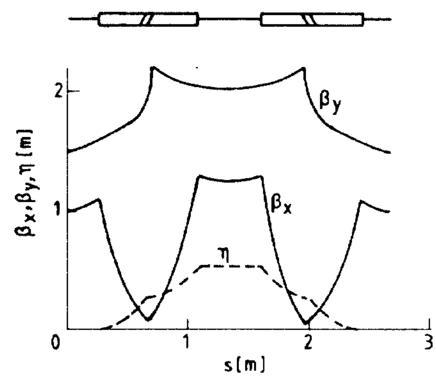

Fig. 4: Dispersion and beta functions at 15 MeV.

An alternative to these gullies is the introduction of weak focussing, the field falls off to the outside. A field of the shape $B(x) = B_o(1-\alpha x^2)$, where x is the horizontal coordinate, and where α is a positive constant, provides elliptical orbits (6) with ν_r = 1 and with positive ν_z. However focussing is weaker than with gullies, and the isochronization is more difficult.

Phase stability and isochronism

The present microtron parameters require 17 RF wavelengths on the first turn, corresponding to an injector energy of about 5 MeV, and one wavelength difference between successive turns.

For energies from 5 to 10 MeV there still is a noticable variation in $\beta = v/c$. A computer program was written for studying phase stability in the presence of phase deviations of the reference particle due to the variation in β and due to field changes. It shows that adiabitic phase changes are allowed. For homogenous fields the initial phase w.r.t. the RF and the injection energy were found by decelerating ("tracing backwards") the reference particle which has a constant synchronous phase ϕ_s for energies above 30 MeV, e.g. $\beta = 1$ would require $\phi_s = 15^o$ and E_{inj} = 5.204 MeV. However since $\beta \neq 1$, $\phi_{inj} = 13.35^o$ and E_{inj} = 5.171 MeV in order to reach $\phi_s = 15^o$ for higher energies. Phase and energy oscillations follow the adiabatic changes.

The corrector coils in the pole piece valleys are used for turn by turn adjustment of the synchronism. The angle kick due to these coils is counter balanced by sets of coils at the exit and entrance of the upper 90° bends. For the 15 MeV orbit in the 25 MeV operation mode a kick of 10 mrad is obtained with 10 mT over 5 cm. This leads to a length variation of 5 mm i.e. to a phase change of 18°.

Pulse selection

When no pulse selection is applied there are 21 pulses simultaneously in the cavity for 20 turns. With 1 out of 2 pulsing there are successively 11 and 10 pulses in the cavity. Overlapping pulses increase space charge effects. The optical cavity of the FEL of 2.5 m long allows a pulse selection as high as 1 out of 50. For pulsing at 1 out of 46 there are no full bunches on top of each other in the RF straight section; the sequence of full and empty periods in the cavity is given in table 2. Pulse selection at 1 out of 23 gives at most two overlapping pulses.

Table 2: Pulse selection at 1 out of 46

A	B	A	B	A	B	A	B
1	1	13	0	25	0	37	1
2	0	14	1	26	1	38	0
3	1	15	0	27	0	39	1
4	0	16	0	28	1	40	0
5	1	17	0	29	1	41	0
6	1	18	0	30	0	42	1
7	1	19	1	31	1	43	1
8	1	20	1	32	1	44	0
9	1	21	0	33	0	45	0
10	0	22	0	34	0	46	1
11	0	23	1	35	0		
12	0	24	1	36	0		

A = RF wave number;
B = number of pulses simultaneously in the cavity

Space charge effects

For an optimal operation of the free electron laser, a beam with high intensity (20-100 A in the micro-pulse), low energy spread ($\Delta E/E \simeq 10^{-3}$) and small emittances ($\epsilon_x \simeq \epsilon_y \simeq 2$ mmmrad) is required. It may be expected that under such conditions space charge effects will become important. In Ref. (7) we presented an analytical model for the calculation of space charge effects in an AVF cyclotron. The method used can also be applied to other types of circular accelerators like the microtron. The model takes into account a special feature of circular accelerators namely the radial-longitudinal coupling which results from the dispersion in the bending magnets. The model is based on the RMS approach (8); it assumes linear space charge forces in the bunch (as determined by a least squares method) and it assumes an ellipsoidal charge distribution. The ellipsoid is allowed to be rotated around its vertical axis because the radial-longitudinal coupling may destroy the symmetry of the bunch with respect to the equilibrium orbit.

The model as given in Ref. (7) ignores the acceleration process. For the isochronous cyclotron this is not a bad approach because then, there is no RF-focussing in the longitudinal phase-space. In the microtron, acceleration essentially influences the motion of individual particles in the bunch due to the longitudinal RF-focussing, i.e. the particles execute synchrotron oscillations around a synchronous phase. We included this effect by adding to the Hamiltonian for the motion of a single particle (given by Eq. (1) in Ref. (7)) an extra longitudinal focussing term given by:

$$+\frac{1}{2} Q_s \bar{s}^2 \quad ; \quad Q_s = \frac{\beta}{2\pi} \frac{1}{\gamma^2 - 1} \frac{\cos\phi_s}{\sin\phi_s} \qquad (1)$$

where $\bar{s}$ is the (scaled) longitudinal coordinate, β the harmonic number of the microtron, γ the relativistic factor and ϕ_s the synchronous phase (since we are above transition the phase ϕ_s has to be chosen such that Q_s is negative). We note that the RF-foccusing does not act continuously around the orbit but only locally at the position of the cavity. Therefore the synchrotron motion has to be described by difference equations instead of differential equations. The representation of Eq. (1) in fact gives a smooth approximation of this stepwise longitudinal motion.

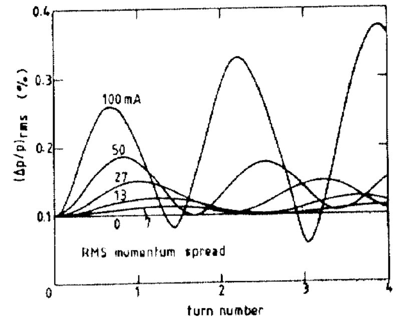

Fig. 5: Time evolution of long. RMS momentum spread of the bunch in the microtron for different values of the av. beam current ϵ_z = 2 mmmrad; ϵ = 2.92 mmmrad; τ = 4.1 (mmmrad)^2; ν_z = 0.1; ν = 1.0; $\bar{B}$ = 0.2 T; r_o = 40 cm; E = 23 MeV).

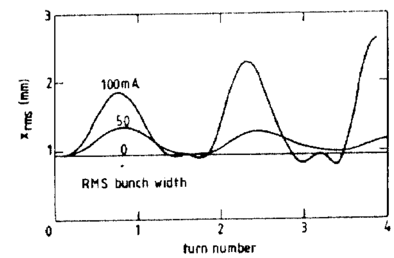

Fig. 6: Time evolution of radial RMS-width of the bunch in the microtron (parameters as in Fig. 5).

As an illustration we give in Fig. 5 and in Fig. 6 some results calculated for a circular microtron. We assumed a magnetic field value $\bar{B}$ of 0.2T, a horizontal tune ν_r equal to unity and a vertical tune ν_z equal to 0.1. We calculated the time evolution of the bunch during four turns. We assumed a constant energy of 23 MeV ($\gamma \simeq 46$, radius $r_o \simeq 40$ cm) but did take into account the RF-focussing according to Eq. (1). The initial conditions were taken such that the properties of the bunch would be stationary in the absence of space charge effects. The solutions are characterized by three constants of motion namely ϵ_z,ϵ and τ. Here ϵ_z is the vertical RMS-emittance which is chosen equal to 2 mmmrad. The quantity ϵ can be considered as a "combination" of radial and longitudinal emittances and is defined in Ref. (7). The constant of motion τ gives the RMS-representation of the 4-dimensional horizontal phase-space volume. We chose $\tau \simeq 4$ (mmmrad) and $\epsilon \simeq 3$ mmmrad.

In Fig. 5 we give the longitudinal momentum spread (FWHM) of the bunch for different values of the average beam current I. The value I = 100 mA corresponds with a peak current in the bunch of ca. 100 A. In Fig. 6 we give the radial RMS-width of the bunch. A comparison of both figures shows that an increase of momentum spread simultaneously gives a broadening of the bunch in the radial direction. This is due to dispersion of the particles. Due to the longitudinal-transverse coupling the time evolution of the properties of the bunch may become rather complicated. A better understanding may be obtained by applying an appropriate canonical transformation on the unperturbed Hamiltonian such that the coupling between the two degrees of freedom is removed. This has not yet been done but nevertheless we can conclude that at peak currents of 100 A space charge will be important. In view of the desired beam quality and intensity it will be necessary to study the problem also numerically with many-particle codes.

References

[1] J.I.M Botman, H.L. Hagedoorn, Proc. 1987 IEEE Part. Acc. Conf., 488
[2] J.S. Fraser, et. al., Proc. 1987 IEEE Part. Acc. Conf. 1705
[3] L.J. Adamski, et. al., IEEE Trans. Nucl. Sci. NS32 No. 5 (1985) 2994
[4] H. Herminghaus, et. al., Nucl. Instr. Meth. 138 (1976) 1
[5] A. Roberts, Ann. Phys. (USA) 4 (1958) 115
[6] J. Botman, EUT Note 1988
[7] W. Kleeven, H.L. Hagedoorn, these proceedings.
[8] F.J. Sacherer, IEEE Trans. Ncul. Sci. 18, 1105 (1971).